Available online at www.sciencedirect.com
ScienceDirect
Journal of Nutritional Biochemistry 21 (2010) 405–412
Journal of Nutritional Biochemistry

Diallyl disulfide causes caspase-dependent apoptosis in human cancer cells through a Bax-triggered mitochondrial pathway

Nagathihalli S. Nagaraj[a,*], Kandangath R. Anilakumar[b], Om V. Singh[c]

[a]Division of Surgical Oncology, Department of Surgery, Vanderbilt University School of Medicine, Nashville, TN 37232, USA
[b]Division of Biochemistry and Nutrition, Defense Food Research Laboratory, Mysore, 5700011 Karnataka, India
[c]Division of Biological and Health Sciences, University of Pittsburgh, Bradford, PA 16701, USA

Received 23 February 2008; received in revised form 19 January 2009; accepted 20 January 2009

Abstract

Diallyl disulfide (DADS), an important component of garlic (*Allium sativum*) derivative, has been demonstrated to exert a potential molecular target against human cancers. We investigated DADS-induced expressions of Apaf1, cystatin B, caspase-3 and FADD (*f*as-*a*ssociated protein with *d*eath *d*omain) in breast, prostate and lung cancer cells. These showed coincident data when further examined by quantitative reverse transcription–polymerase chain reaction and Western blot analysis. Furthermore, DADS induced a marked amount of Bax translocation, cytochrome *c* release and activation of caspase-3 and caspase-9. DADS-treated tumor cells triggered mitochondria-mediated signaling pathways that led to a significant increase in apoptosis induction. Further studies with caspase-3 and caspase-9 inhibitors (zDEVD-fmk and zLEHD-fmk, respectively) proved that DADS induces apoptosis through a caspase-3-dependent pathway. DADS is only an agent used in the study. The molecular mechanism presented therefore provides strong additional support to the hypothesis that DADS is a strong inducer of apoptosis through a Bax-triggered mitochondria-mediated and caspase-3-dependent pathway. This study shows clearly that DADS causes caspase-dependent apoptosis in human cancer cells through a Bax-triggered mitochondrial pathway. Therefore, the mitochondrial pathway might be the target for cancer chemoprevention and/or chemotherapy by DADS.
Published by Elsevier Inc.

Keywords: Diallyl disulfide; Garlic; Apoptosis; Caspase-3; Mitochondria; Tumor

1. Introduction

For centuries, garlic has been used in disease prevention and treatment by several ethnic cultures. In vitro and in vivo studies provide convincing evidence that garlic and some of its organosulfur components are effective inhibitors of a variety of cancers, including breast, colon, skin, uterine, esophageal, prostate and lung cancers, and neuroblastoma [1–5]. However, the specific component(s) of garlic that underlies specific cellular and molecular events governing anticancer properties is not known with certainty. The allyl sulfur compounds formed by enzymatic activity when garlic is minced or crushed — such as allicin; water-soluble *S*-allylmercaptocysteine and *S*-allylcysteine; and oil-soluble diallyl disulfide (DADS), diallyl trisulfide and diallyl sulfide — probably account for the majority of these anticancer effects [6–9]. DADS is one of the most abundant oil-soluble garlic derivatives, with several beneficial properties. It has been reported that DADS can decrease the risk of hypertension and coronary diseases owing to its inhibitory action on plaque formation [10] and cholesterol synthesis [11]. Moreover, it has been shown that DADS has both antioxidant and anticancer properties. A low concentration of DADS could be a potential therapeutic or modulating agent for neurodegenerative and other diseases associated with oxidative damage, whereas a high concentration of DADS could be a powerful tool against proliferation through induction of apoptosis in cancer cells.

Apoptosis in response to cancer therapy proceeds through activation of the core apoptotic machinery, including the extrinsic cell death receptor and the intrinsic mitochondrial signaling pathway [12]. The major regulators of the intrinsic pathway are the pro-death and anti-death members of the Bcl-2 family [13]. The intrinsic pathway is characterized by mitochondrial dysfunction with release of caspase activators, including cytochrome *c*, followed by activation of caspase-9 and caspase-3 [14]. In certain cell types, caspase-8 has been shown to convert Bid from a latent proapoptotic form into a strongly proapoptotic form capable of inducing cytochrome *c* release through the action of Bax or Bak and subsequent activation of caspase-9 [15]. This release of cytochrome *c* into the cytosol triggers caspase-3 activation through formation of the cytochrome *c*/Apaf1/caspase-9 apoptosome complex. Upon triggering, caspases (the final executioners of apoptosis) are activated, causing degradation of cellular

* Corresponding author. Tel.: +1 615 509 1565; fax: +1 615 322 6174.
E-mail addresses: nagaraj.nagathihalli@vanderbilt.edu, nagarajns@hotmail.com (N.S. Nagaraj).

0955-2863/$ – see front matter. Published by Elsevier Inc.
doi:10.1016/j.jnutbio.2009.01.015

proteins and leading to typical morphological changes such as chromatin condensation, nuclear shrinkage and formation of apoptotic bodies [15]. Therefore, inducing the apoptosis of cancer cells is a major strategy for cancer chemotherapy.

Under physiological conditions, Bax is a cytosolic protein. However, upon apoptosis induction, Bax inserts into the outer mitochondrial membrane [16], where it is thought to form supramolecular openings alone or in association with other proapoptotic members such as Bak or tBid (truncated Bid) [17]. Such openings might result from formation of homooligomeric Bax-containing pores or from destabilization of the lipid bilayer, resulting in transient discontinuities within the outer mitochondrial membrane. Bax and Bak "find their way" to the mitochondria, and whether they are attracted through specific properties of the lipid or protein composition is not very well known [18]. Reportedly, large Bax oligomers organize in clusters near the mitochondria shortly after their translocation to the mitochondria [19]. How the molecular openings induced by Bax/Bak and/or Bax/tBid mediate cytochrome *c* release is still a highly questionable issue. The cytosolic release of cytochrome *c* is one of the key events in the mitochondria-dependent apoptotic pathway [18]. The up-regulation of Bcl-2 (and of other antiapoptotic members of the Bcl-2 family) and/or the down-regulation of Bax has been reported in several clinical studies of cancer patients and, notably, in a high proportion of hematopoietic and lymphoid neoplasms [18]. Obviously, these changes may be directly related to regulation of mitochondrion membrane permeabilization. Impaired mitochondrion membrane permeabilization may lead to invalidation of the apoptotic response found in cancer [20,21]. Currently, more than 20 mitochondrion-targeted compounds have been reported to induce apoptosis selectively in malignant cell lines, and some of these are already being used in phase II/III clinical trials or are being validated in vitro in preclinical settings [22,23].

Even though recent studies have shown that DADS induces apoptosis in human leukemia and colon, prostate and breast cancer cells [8], knowledge of the mechanism of the cancer chemopreventive effect of DADS is limited. Our studies address the molecular mechanism of DADS that affects the apoptosis of different human tumor types. We showed that DADS induced apoptosis independently by affecting the mitochondria and by subsequently activating the caspase-3 pathway in human tumor cells.

2. Materials and methods

2.1. Cell culture and treatment

Breast (MCF-7), prostate (PC-3) and lung (Calu-1) cancer cells were obtained from the American Type Culture Collection (ATCC; Rockville, MD). The other cell lines used in our study were HCT-116, DLD-1 and HCT-15 from colon cancer, and A549, H460 and H1299 from lung cancer. Cells were cultured in accordance with ATCC instructions. The medium was supplemented with 10% fetal bovine serum and 1% penicillin/streptomycin and maintained in 5% CO_2, 95% air and 37°C. Treatments were performed with different amounts of DADS ($C_6H_{10}S_2$) (Sigma, St. Louis, MO) ranging from 5 to 200 μM at 37°C in a medium supplemented with serum. Unless specified, the concentration of DADS selected for all the experiments was 50 μM because it gives a valuable degree of apoptosis in these tumor cells and because it is within the range used for in vivo studies [24]. As control, an equal amount of DMSO was added to untreated cells.

2.2. RNA isolation and cDNA synthesis

Cells were grown to approximately 75% confluence in six-well plates, with or without DADS treatment (50 μM, 12 h), and total RNA was isolated with TriZol reagent (Invitrogen Corporation, Carlsbad, CA). The purity and integrity of each RNA preparation were evaluated using RNA Nano Chips on an Agilent 2100 Bioanalyzer (Agilent Technologies, Palo Alto, CA). First-strand cDNA was synthesized using the SuperScript First-Strand Synthesis kit (Invitrogen Corporation). DNA contamination was monitored in our RNA samples by 'no-reverse-transcriptase' reactions performed in conjunction with cDNA synthesis reaction.

2.3. Quantitative reverse transcription–polymerase chain reaction

The specificity of the amplified product was confirmed with (quantitative) melting curve analysis. Two microliters of cDNA was amplified in 5 μl of 10× PCR buffer, 5 μl of 25 mM $MgCl_2$, 1 μl of 10 mM dNTP, 1 μl of 0.2 μM each oligonucleotide primer and 1 μl of 1.25 U of Taq DNA polymerase, and water up to 50 μl. RT-PCR cycles consisted of initial denaturing for 10 min at 95°C, followed by 40 cycles of denaturation at 95°C/10 s, annealing at 65°C/30 s and extension at 72°C/40 s for Apaf1, cystatin B, caspase-3, caspase-2, FADD (*fas*-associated protein with *d*eath *d*omain), CK8 and S1000A11. The PCR conditions for β-actin were (94°C for 10 min, 94°C for 1 min and 55°C for 45 s) ×35 cycles. DNA final extension was carried out at 72°C for 10 min. β-Actin amplification was used as internal control. Relative quantitation of Apaf1, cystatin B, caspase-3, caspase-2, FADD, CK8 and S1000A11 quantitative reverse transcription–polymerase chain reaction (qRT-PCR) was performed using an ABI PRISM 7700 Sequence Detection System (Applied Biosystems, Foster City, CA). The cDNA prepared was diluted to 1 ng/μl, and 2 μl was used as template for qRT-PCR in a 25-μl reaction. A forward primer–reverse primer mix was added (3 μl, 1:1 mix, 0.3 μM each) in SYBR Green PCR Master Mix (Applied Biosystems). Each reaction was performed in triplicate, and 'no-template' controls were included in each experiment. Dissociation curves were run to eliminate nonspecific amplification, including primers–dimers. Cycle threshold (C_T) values were normalized to the housekeeping gene *β-actin*, and fold change was calculated using the $2^{-\Delta\Delta C_T}$ method.

DNA primers for RT-PCR were used as follows: Apaf1 forward (5′-ATG-AGA-GTT-TTT-CCC-AGA-GGC-TTC-3′) and reverse (5′-TTG-AGG-TAG-TAC-TCC-CAG-CGA-TTG-3′), caspase-2L forward (5′-ATG-GCC-GCT-GAC-AGG-GGA-CGC-3′) and reverse (5′-GGC-AGC-AAG-TTG-AGG-AGT-TC-3′), cystatin B forward (5′-CGT-GGG-TGG-GGT-GAA-CTA-CTA-3′) and reverse (5′-TTT-GGC-TGG-TCA-TTG-AAG-GGA-3′), caspase-3 forward (5′-CTC-GGT-CTG-GTA-CAG-ATG-TCG-ATG-T-3′) and reverse (5′-GGT-TAA-CCC-GGG-TAA-GAA-TGT-GCA-3′), FADD forward (5′-AAA-GTC-TCA-GAC-ACC-AAG-ATC-GAC-A-3′) and reverse (5′-GCA-CCT-CAC-AGA-TAT-TAT-CTC-AAT-TCG-3′), CK8 forward (5′-GGA-GGC-ATC-ACC-GCA-GTT-AC-3′) and reverse (5′-GGT-TGG-CAA-TAT-CCT-CGT-ACT-GT-3′), and S100A11 forward (5′-CTG-AGC-GGT-GCA-TCG-AGT-C-3′) and reverse (5′-TGT-GAA-GGC-AGC-TAG-TTC-TGT-A-3′), and endogenous control β-actin primers were designed using the PrimerBank software (http://pga.mgh.harvard.edu/primerbank/).

2.4. Protein extraction and Western blot analysis

Treated or control cells were rinsed with ice-cold PBS, scraped into 1 ml of PBS and centrifuged at 4000 rpm for 3 min. The pellets were resuspended in RIPA buffer [10 mM Tris–HCl (pH 7.4), 150 mM NaCl, 1% Triton X-100, 0.1% sodium dodecyl sulfate (SDS) and 1 mM EDTA] containing protease inhibitors (0.5 mM phenylmethylsulfonyl fluoride, 10 μg/ml aprotinin and 2 μg/ml of both leupeptin and pepstatin). Then cell extracts were sonicated, and cell debris was removed by centrifugation. To obtain cellular proteins for cystatin B, cells were washed in ice-cold PBS and extracted using M-PER Mammalian Protein Extraction Reagent with protease inhibitor cocktail. Proteins were quantified using the Bradford protein assay kit and compared with a γ-globulin standard curve. Equal amounts of total proteins were separated on an SDS polyacrylamide gel and transferred onto nitrocellulose membranes by electroblotting overnight at 20 V. Membranes were blocked in TBS-T (10 mM Tris–HCl, 150 mM NaCl and 0.25% Tween 20, pH 7.5) with 5% fat-free powdered milk at room temperature for 1 h. After the membrane had been rinsed in TBS-T, the following primary antibodies were used: rabbit or goat polyclonal IgG for Apaf1, FADD, cystatin B, caspase-9 and caspase-3, or mouse monoclonal IgG for p53, Bcl-2 and β-actin antibodies. After overnight incubation at 4°C or for 1 h at room temperature, the membranes were washed four times (10 min each) in TBS-T. The secondary antibodies used were either horseradish-peroxidase-conjugated goat anti-rabbit IgG or goat anti-mouse IgG, followed by five washes with TBS-T. Bands were detected using ECL substrate. For β-actin detection, previously probed membranes were soaked in stripping buffer [70 mM Tris–HCl (pH 6.8), 2% SDS and 0.1% β-mercaptoethanol] at 60°C for 30 min and incubated as above.

2.5. Caspase activity assay

Cells were grown in six-well plates to 50–60% confluence and treated with DADS with or without pretreatment with zDEVD-fmk (20 μM) or zLEHD-fmk (20 μM). Then cells were rinsed once and collected in cold PBS by scraping. Cell samples were prepared as described previously [25]. The peptide substrates for caspase-3 and caspase-9 assays were Ac-DEVD-AFC and Ac-LEHD-AFC, respectively, each dissolved in dimethyl sulfoxide; the respective specific inhibitors DEVD-CHO and LEHD-CHO were used in control reactions. Assays were performed in black-wall clear-bottom plates using a Spectramax Gemini XS Microplate Spectrofluorometer (Molecular Devices, Sunnyvale, CA). Reading was performed at 500 nm after excitation at 405 nm had been determined for AFC. The results were compared against AFC standard curves generated in parallel. Specific activity was expressed as units, with 1 U defined as an AFC release of 1 nmol/h/μg protein. Ac-DEVD-AFC and DEVD-CHO were purchased from Alexis (San Diego, CA), and LEHD-CHO and Ac-LEHD-AFC were purchased from Biomol (Plymouth Meeting, PA).

2.6. Mitochondrial membrane potential ($\Delta\psi_m$) assessment

Mitochondrial membrane potential $\Delta\psi_m$ was assessed using a dye, 5,5′,6,6′-tetrachloro-1,1′,3,3′-tetraethylbenzimidazolyl-carbocyanine iodide (JC-1; Molecular Probes, Eugene, OR), after DADS exposure, followed by fluorescence-activated cell sorting (FACS) analysis for red and green fluorescence. The cells were stained with JC-1 for 15 min at 37°C in a 5% CO_2 incubator, rinsed with assay buffer and examined by flow cytometry. The JC-1 monomer was detected in the flow cytometer for red fluorescence channels. Red fluorescence was expressed as a percentage of total gated cells.

2.7. Immunfluorescence localization of caspase-3

Cells were grown on sterile glass cover slips and treated with or without DADS (50 μM). Following treatments, the cells were washed in PBS and fixed in 2% paraformaldehyde in PBS for 15 min. After the cells had been washed twice in PBS, they were permeabilized with 0.2% Triton X-100 for 10 min and in blocking buffer containing 3% bovine serum albumin in PBS for 1 h. The cells were then incubated with mouse anti-caspase-3 (active) antibodies (Santa Cruz Biotechnology, Santa Cruz, CA) (1:200) for 1 h at 37°C in a humidified incubator. After three washes in PBS containing 1% bovine serum albumin, the cells were incubated at 37°C in a humidified incubator for 1 h with a 1:500 dilution of Alexa-Fluor-conjugated secondary antibody in blocking solution and again washed with PBS. The nuclei were stained with 0.5 μg/ml 4′,6′-diamidino-2-phenylindole for 5 min, and the cells were washed twice in PBS. Coverslips were then mounted on slides using antifade mounting medium (Molecular Probes). Localization of active caspase-3 and morphological changes in the nuclei were analyzed using a Nikon Inverted Microscope Eclipse TE300, and images were captured by a cool-snap HQ digital B/W CCD camera (Roper Scientific, Trenton, NJ). Images shown are representative of at least three independent studies.

2.8. Cell fractionation and mitochondria isolation

Crude mitochondria and cytosolic extracts were prepared from cells as described previously by Parone et al. [26]. In brief, cells were mechanically broken three times using a homogenizer. Homogenates were cleared at 1500×*g*, and mitochondria were spun down at 10,000×*g*. Protein concentrations were measured with a Bradford assay (Bio-Rad Laboratories). Proteins in the supernatants (cytosolic fractions) were precipitated with 10% trichloroacetic acid (TCA) (for 30 min on ice). Either samples were directly analyzed by immunoblotting or mitochondria were processed for further tests. Western blot analysis for cytochrome *c* was performed with mouse monoclonal anti-cytochrome *c* IgG (BD Biosciences-Pharmingen, San Diego, CA), and that for Bax was performed with rabbit polyclonal anti-Bax (Santa Cruz Biotechnology), and the absence of intramitochondrial proteins was verified by blotting for mitochondrial cytochrome oxidase (COX) with mouse monoclonal anti-COX4.

2.9. Determination of apoptosis

Cells were treated with DADS and/or caspase inhibitors as described above. Apoptosis detection by FACS analysis was performed after the cells had been stained with propidium iodide (Invitrogen Corporation). Cells were trypsinized, washed and resuspended in cold PBS. After centrifugation at 1000 rpm for 5 min, 5×10^5 cells were fixed with 1 ml of 70% ethanol at −20°C and washed with PBS. Each pellet was resuspended in 500 μl of propidium iodide buffer (20 μg/ml propidium iodide and 10 mg/ml RNase in PBS). After incubation for 30 min in the dark at room temperature, cell fluorescence signals were determined using a FACScalibur flow cytometer (BD Biosciences, San Jose, CA) and analyzed with its CellQuest software. Cells to the left of the first peak at sub-G1 contained hypodiploid DNA, were considered apoptotic and were expressed as a percentage of total gated cells.

2.10. Statistical analysis

Data from viability, qRT-PCR, Western blot analysis, enzyme activity and FACS assays were derived from at least three independent experiments. Statistical analyses were conducted using the Prism4 and InStat3 GraphPad software, and values were presented as mean±SD. The significance level was calculated using one-way analysis of variance to assess the differences between experimental groups.

3. Results

3.1. Apoptosis-associated expression analysis of up-regulated or down-regulated genes and proteins in DADS-treated tumor cells

mRNA expression analysis was performed on tumor cells for Apaf1, cystatin B, caspase-3, FADD, CK8 and S100A11, which were selected based on our earlier work with expression analysis by genomic and proteomic methods [27]. Considering the significant role played by Apaf1, caspase-3 and FADD in apoptosis [28–30], we explored the possibility that DADS could induce apoptosis in tumor cells. To investigate whether DADS stimulates this expression in tumor cells in mRNA, real-time qRT-PCR analysis using gene-specific primers was performed after exposure of the MCF-7, PC-3 and Calu-1 cells to DADS (50 μM) for 12 h (Fig. 1A). Apaf1, cystatin B, caspase-3, FADD, CK8 and S100A11 were induced by DADS treatment. Interestingly, Apaf1, caspase-3, FADD and S100A11 were up-regulated (~2- to 11-fold), and cystatin B and CK8 were down-regulated (~2- to 7-fold) in DADS-treated cells compared to control cells (Fig. 1A).

Induction by DADS (50 μM, 12 h) was further confirmed by protein expression analyses using Western blot analysis (Fig. 1B). The levels of β-actin were monitored to ensure equal loading of protein samples. Treatment with DADS increased the expression levels of Apaf1, caspase-3 and FADD, and decreased the levels of cystatin B in the cell lines studied, correlating with our qRT-PCR data (Fig. 1A). The proform of caspase-3 was cleaved after DADS treatment (Fig. 1B), accompanied by an increase in caspase-3-like activity (Fig. 2A), indicating that the decrease in pro-caspase-3 resulted from enzyme activation. FADD and Apaf1 were released in large amounts after DADS treatment. The increase in these apoptosis markers was one of the greatest changes observed when all these were analyzed in tumor cells.

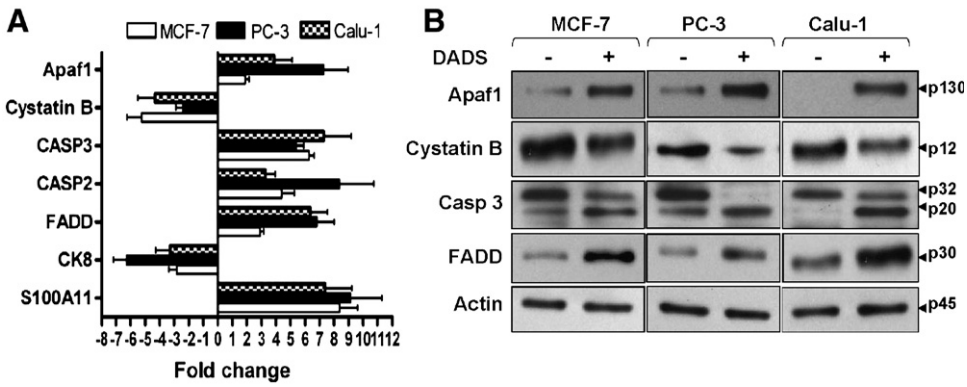

Fig. 1. DADS stimulates Apaf1, cystatin B, caspase-3 and FADD mRNA and protein expressions in tumor cells. (A) The total RNA preparations from control and DADS-treated (50 μM, 12 h) cells were subjected to real-time qRT-PCR using primers specific for Apaf1, cystatin B, caspase-3, caspase-2, FADD, CK8 and S100A11, and the internal standard control β-actin. Fold change levels are relative to the expression in cell samples. Results are presented as the mean±SD of three independent assays. (B) The cell protein preparations from control and DADS-treated (50 μM, 12 h) cells were subjected to immunoblot analysis using specific antibodies for Apaf1, cystatin B, caspase-3 and FADD, and the internal standard control β-actin. Individual blots show release of Apaf1 (130 kDa), decrease in cystatin B (12 kDa), processing of caspase-3 (32 kDa) into active form (20 kDa) and release of FADD (30 kDa). Reprobing for β-actin (45 kDa) antibody was used as control to determine equal protein loading for each sample. Data are representative of two independent experiments with similar results.

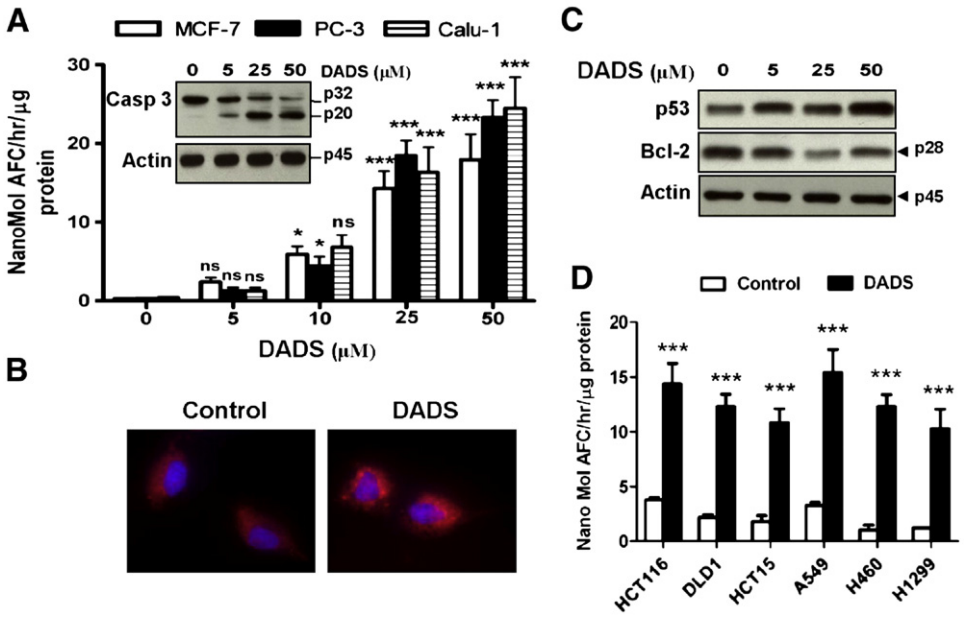

Fig. 2. Dose-dependent changes in the levels of p53, Bcl-2 and caspase-3 in tumor cells treated with DADS. (A) Caspase-3 activity was measured by using specific fluorometric substrates, as described for MCF-7, PC-3 and Calu-1 cells in Materials and Methods. Western blot analysis of MCF-7 cells (A; insert) showing cleavage of pro-caspase-3 (32 kDa) into the active (20 kDa) form. Reprobing for β-actin served as internal loading control. Western blot data are representative of two independent experiments with similar results. (B) Cleaved caspase-3 was detected by indirect immunofluorescent labeling in MCF-7 cells with or without DADS (50 μM, 12 h) treatment. (C) The tumor cell line MCF-7 was treated with 0, 5, 25 and 50 μM DADS for 12 h, then cytosolic fractions were subjected to immunoblot analysis using specific antibodies. Evaluation of the levels of p53 (53 kDa) and Bcl-2 (28 kDa) expressions was estimated by Western blot analysis, as described in Materials and Methods. Reprobing for β-actin served as internal loading control. (D) Caspase-3 activity was measured using specific fluorometric substrates, as described for HCT116, DLD1, HCT15, A549, H460 and H1299 cells in Materials and Methods. The activity results shown in (A) and (D) are presented as the mean ±SD from three separate experiments; the significance of DADS-treated cells was compared with that of untreated controls. *P<.05, **P<.01 and ***P<.001; all others are nonsignificant.

3.2. Dose dependence changes in caspase-3, p53 and Bcl-2 in DADS-treated tumor cells

The activation of caspase-3 is a key event in apoptosis. Caspase-3 activity significantly (P<.001) increased from a concentration of 25 μM onwards in the MCF-7, PC-3 and Calu-1 cell lines (Fig. 2A). Western blot analysis of caspase-3 protein was performed using a specific antibody that recognizes the pro and activated forms of caspase-3 (Fig. 2A, insert). The DADS-induced proteolytic cleavage of procaspase-3 occurs in a dose-dependent manner in MCF-7 cells. The caspase-3 activity was maximal at 12 h and preceded apoptosis, consistent with other reports indicating that caspase-3 activation is required for apoptosis. We also examined the effects of DADS on caspase-3 activation by immunofluorescence with mouse anti-caspase-3 (active) antibody. We showed the activation of caspase-3 in the MCF-7 cells treated with DADS (Fig. 2B), consistent with the caspase-3 activity results. Next, Western blot analysis was performed to examine the expressions of Bcl-2 and p53 that participate in cell apoptosis in a dose-dependent pattern (Fig. 2C). β-Actin expression was monitored to ensure that equal amounts of cytosolic protein samples were loaded. A change in the levels of expression of proapoptotic p53 and antiapoptotic Bcl-2 proteins resulted in a significant change in the levels of apoptosis. Expression of Bcl-2 decreased, and expression of p53 increased significantly when treated with DADS in tumor cells (Fig. 2C). Caspase-3 activities were compared in different tumor cells exposed to DADS (25 μM) (Fig. 2D). Tumor cell lines were selected based on p53 mutation status. The p53 wild-type cell lines from breast cancer (MCF-7), colon cancer (HCT116 and DLD1) and lung cancer (A549 and H460), and the p53 mutated cell lines from prostate cancer (PC-3), lung cancer (Calu-1 and H1299) and colon cancer (HCT15) were selected. When these cells were exposed to DADS, caspase-3 activity increased very significantly (P<.001) irrespective of the p53 mutation status.

3.3. Alteration in apoptosis markers during DADS-induced apoptosis

The purpose of these experiments was to examine whether or not caspase-3 activation is involved in the apoptosis of tumor cells triggered by DADS. Bax translocation from the cytosol to mitochondria has been observed in mammalian cell lines exposed to various apoptotic stimuli. We have demonstrated that endogenous Bax protein translocated from the cytosol to the mitochondria, specifically during apoptosis induced by DADS (50 μM) (Fig. 3A). The Bax expression level in the mitochondrial fraction increased, whereas it decreased in the cytosolic fraction with DADS treatment (Fig. 3A). The mitochondrial matrix protein COX4 was used to ascertain the purity of the fractions. COX4 was unchanged in the mitochondrial fraction. A change in Bax/Bcl-2 determines the commitment of cells to triggering mitochondrial release of cytochrome *c* into the cytosol. We then measured the extent of mitochondrial release of cytochrome *c* using a subcellular fractionation method. As shown in Fig. 3A, treatment of tumor cells with DADS induced the release of cytochrome *c* from the mitochondria to the cytosolic compartment. Through loss of their membrane potential, the mitochondria have a prominent role in the apoptotic process by releasing proapoptotic factors such as cytochrome *c* from their intermembrane space into the cytoplasmic compartment. Thus, the mechanism of apoptosis involved the mitochondrial release of cytochrome *c*, which could cause subsequential activation of caspase-9 and caspase-3. DADS treatment resulted in cleavage of the 47-kDa procaspase-9 (Fig. 3A) to yield fragments in parallel to caspase-3 cleavage (Fig. 1B) with the use of whole cell lysates. Caspase-3, a prevalent caspase, is ultimately responsible for the majority of apoptotic processes. Therefore, DADS-induced Bax translocation is accompanied by activation of caspase-3. These results suggest that differences in the role of mitochondria and activation of caspase-3 may play a role in the process of apoptosis induced by DADS.

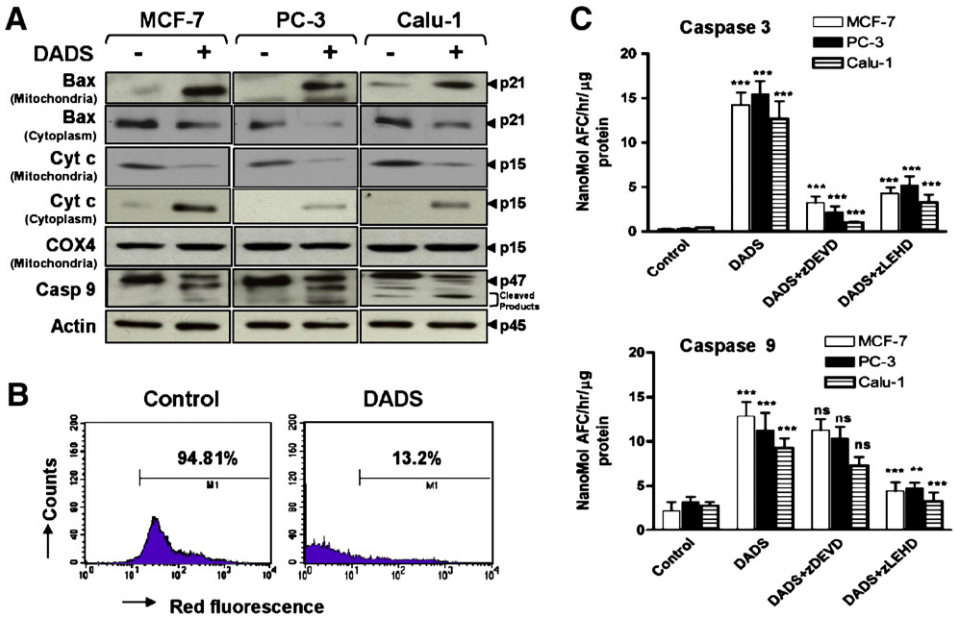

Fig. 3. Change in apoptosis markers in DADS-treated tumor cells. MCF-7, PC-3 and Calu-1 cells were exposed to DADS (50 μM, 12 h) as described in Materials and Methods. (A) Western blot analysis of tumor cells treated with DADS showing Bax (21 kDa) translocation from the cytosol to the mitochondria; cytochrome *c* (15 kDa) release into cytosolic fraction from the mitochondria; COX4 (15 kDa) as mitochondrial control; and cleavage of pro-caspase-9 (47 kDa) into the active forms (whole cell lysate). Reprobing for β-actin served as internal loading control. Western blot data are representative of two to three independent experiments with similar results. (B) Mitochondrial membrane potential ($\Delta\psi_m$) in MCF-7 cells was assessed by using JC-1 dye, and FACS analysis was performed for red fluorescence and expressed as a percentage of total gated cells. (C) Caspase-3 and caspase-9 activities were measured with or without the caspase inhibitors zDEVD-fmk (20 μM) and zLEHD-fmk (20 μM) by using specific fluorometric substrates, as described in Materials and Methods. The activity results shown are presented as the mean±SD from three separate experiments; the significance of DADS-treated cells was compared with that of untreated controls; all other inhibitor-treated cells were compared with DADS treatment. *P<.05, **P<.01 and ***P<.001; all others are nonsignificant.

Loss of mitochondrial membrane potential provides an early indication of the initiation of cellular apoptosis. We measured cellular mitochondrial membrane potential in MCF-7 cells after treatment with DADS (50 μM) (Fig. 3B). We found that DADS strongly induced loss of mitochondrial membrane potential by using JC-1. The loss of mitochondrial membrane potential decreased from 95% in control cells to 13% after treatment with DADS for 12 h. We also observed almost the same amount of effect in other tumor cells (data not shown). This triggers activation of downstream events that lead to apoptosis. Taken together, the loss of mitochondrial membrane

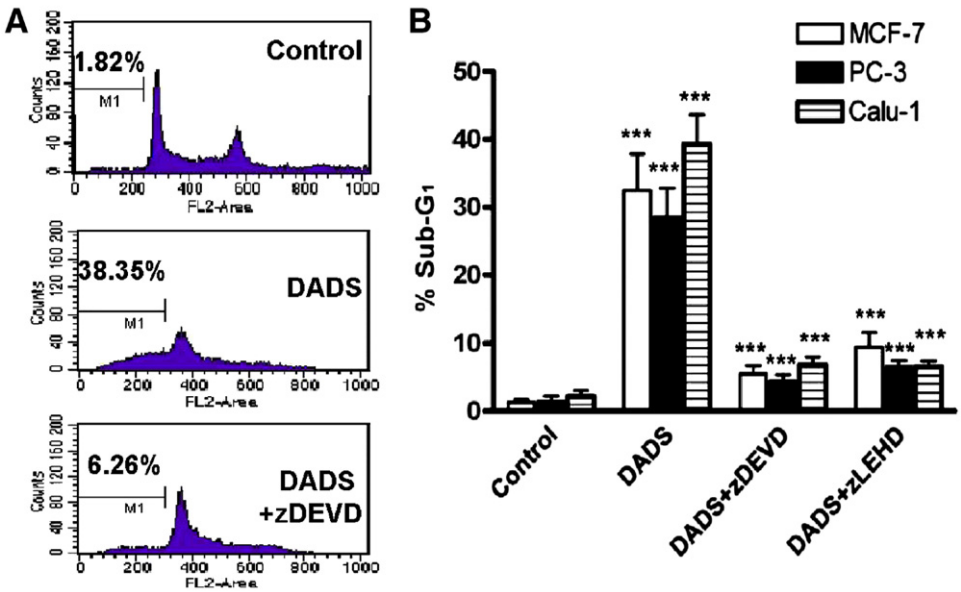

Fig. 4. DADS-induced apoptosis. Tumor cells MCF-7, PC-3 and Calu-1 were exposed to DADS (50 μM) and/or after pretreatment with or without zDEVD-fmk (20 μM) or zLEHD-fmk (20 μM) and analyzed for the percentage of apoptosis. FACS analysis of cells labeled with propidium iodide; apoptotic cells with sub-G1 chromosomal DNA content are expressed as a percentage of total gated cells. (A) MCF-7 cells showing the percentage of apoptosis induction. (B) FACS data of the MCF-7, PC-3 and Calu-1 cells presented as the mean±SD from three separate experiments; the significance of DADS-treated cells was compared with that of untreated controls; all other inhibitor-treated cells were compared with DADS treatment. *P<.05, **P<.01 and ***P<.001; all others are nonsignificant.

potential and the above results suggest that the mitochondrial pathway plays an important role in apoptosis induced by DADS.

Caspase-3 and caspase-9 activities significantly increased with DADS treatment (Fig. 3C). Inhibitors were treated 3 h prior to DADS treatment before being assayed for caspase-3 or caspase-9 activities. We investigated the effects of individual cell-permeable caspase inhibitors on caspase-3 and caspase-9 activities during DADS treatment (Fig. 3C). These inhibitors can enter viable cells and are covalently and irreversibly bound to their target caspases. zDEVD-fmk was an inhibitor of caspase-3, and zLEHD-fmk was an inhibitor of caspase-9. The presence of zDEVD-fmk clearly inhibited the activity of its target protease caspase-3, but not that of caspase-9. zLEHD-fmk as inhibitor for caspase-9 decreased caspase-3 activity, and this shows the downstream effect of caspase-9. These data showed that caspase-9 contributes to caspase-3 activity during DADS treatment, and that these are the main caspases involved in the mitochondria-mediated apoptosis activation pathways of tumor cells.

3.4. DADS-induced apoptosis

Apoptosis was detected by propidium iodide staining after 12 h of continuous exposure to DADS (50 μM) and then analyzed by flow cytometry. As shown in Fig. 4, DADS induced a significant amount of apoptosis compared to control. To investigate the effects of DADS-induced apoptosis morphology, we exposed human tumor cells with DADS with or without addition of caspase inhibitors zDEVD-fmk and zLEHD-fmk. When analyzed by flow cytometry, apoptotic cells with degraded DNA appeared as cells with hypodiploid DNA content, represented in so-called “sub-G1” peaks to the left of the main G1 peak on DNA histograms (Fig. 4A). There was prominent apoptosis induction after treatment with DADS in the cell lines studied. The tumor cells studied were most sensitive to DADS, with 25–45% apoptosis. Clearly, caspase-3 and caspase-9 inhibitors decreased the efficacy of DADS-induced apoptosis rates substantially in the cell lines from 25–45% to 5–10% (Fig. 4B). The protective effects of zDEVD-fmk and zLEHD-fmk on tumor cells exposed to DADS proved the involvement of caspase-3 in DADS-induced apoptosis. These data indicate that DADS generates an apoptotic signal in a caspase-dependent mode and confirms the involvement of caspase-3 in cell death induced by DADS.

4. Discussion

Induction of apoptosis represents a novel mechanism to eliminate precancerous or cancerous cells, therefore contributing to chemoprevention. In this context, many dietary plant constituents were found to induce apoptosis in various cancer cell lines [31,32]. Many investigators have focused on the manipulation of the apoptotic process for the treatment and prevention of cancer, and they have also searched for compounds that influence apoptosis to understand their mechanism of action. DADS is reported to comprise 60% of garlic oil [33], indicating that it is the most appropriate compound for use in the study of the possible effects of raw and cooked garlic. The occurrence of DADS-induced apoptosis has also been reported recently by others [2,24,34].

Recently, our proteomic and genomic assays demonstrated the massive response of protein and gene expressions in cancer cells induced by DADS and demonstrated that numerous DADS-sensitive proteins or genes in these cell lines are related to apoptosis [27]. Interestingly, almost 60–70% of proteins/genes in the MCF-7, PC-3 and Calu-1 cell lines studied are highly associated with the apoptotic pathway. Many of our genomic profiles were in agreement with our proteomic observations. DADS exerts multiple stimuli to several biological pathways, and diverse molecular responses merge into apoptotic pathways that could strengthen anticarcinogenic effects. In the present work, some of the highly regulated genes or proteins were analyzed further. DADS up-regulated Apaf1, caspase-3, FADD and S100A11 expression and down-regulated cystatin B and CK8 gene expression in breast, prostate and lung carcinoma cells. Some of these results were further confirmed in this study by qRT-PCR and Western blot analysis (Fig. 1). Some of the functions of these molecules in the apoptosis pathway are as follows: (a) p53 directly up-regulates Apaf1 transcription as a critical step in the induction of neuronal cell death [35]; (b) FADD, a novel death-domain-containing protein, interacts with the death domain of Fas and initiates apoptosis [36]; (c) S100A11, a putative tumor-suppressor gene, is overexpressed in pancreatic carcinogenesis [37]; and (d) cystatin-B-deficient mice have increased expression of apoptosis [38].

In the present study, the initial results revealed that the p53 protein that increased its expression with DADS treatment may play an important role in the apoptotic response of a cell with DNA damage. The apoptotic effects of anticancer drugs were known to be linked with the expression of oncogenes or tumor-suppressor genes such as *p53* and *Bcl-2*. Consistent with the potential role of p53 in modulating chemotherapy in human cancers, loss of p53 function was linked to chemoresistance in certain tumor types [39–41]. Additionally, p53 seemed to be an important mediator in DADS-induced apoptosis, supported by the evidence that DADS up-regulated p53 in a human wild-type p53 colon cancer cell line but did not affect p53 in its mutant p53 counterpart [42]. Both wild-type p53-containing cell lines (MCF-7, HCT116, DLD1, A549 and H460) and mutated cell lines (PC-3, Calu-1, HCT15 and H1299) showed very high caspase-3 activity when treated with DADS. Bax translocation also occurred irrespective of p53 mutation status. The antiapoptotic activity of Bcl-2 correlates with its intracellular ratio to Bax. High levels of Bax have been shown to favor apoptosis in DADS-treated tumor cells. These results

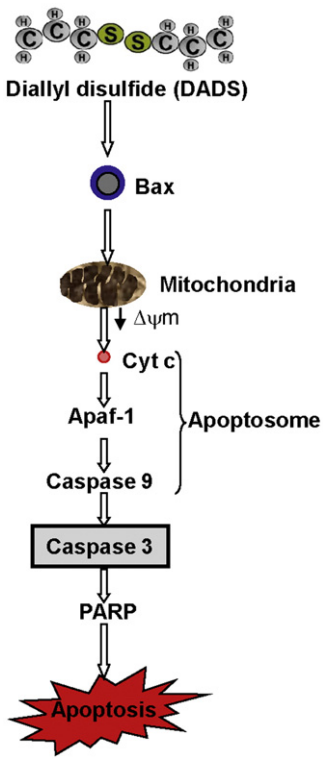

Fig. 5. Model of the molecular mechanisms of DADS-induced apoptosis. DADS activates Bax translocation to mitochondria, promoting cytochrome *c* release from the mitochondria to the cytosol. The apoptosome recruits and processes caspase-9 to form a holoenzyme complex. This cascade activates the downstream executioner caspase-3, resulting in apoptosis.

suggested the possibility that although there may be a correlation between p53 induction and apoptosis under some circumstances, caspase-3 activity and apoptosis induction may provide an independent prediction in DADS-treated tumor cells. This needs further investigation using a larger series of tumor-derived p53 wild-type and mutant cell lines.

Apparently, DADS induces apoptosis through the mitochondrial pathway, as evidenced by the loss of mitochondrial membrane potential and the release of mitochondrial cytochrome *c* (Fig. 3B and C). In the mitochondria-dependent pathway of apoptosis, both cytosolic protein Apaf1 and cytochrome *c* participate in the activation of caspase-9, which in turn processes pro-caspase-3 to generate active caspase-3. Our data showed that DADS-induced cell death was mediated by caspase-9 and caspase-3 activation. Apoptosis was inhibited by the pretreatment of the caspase-3 inhibitor zDEVD-fmk. Using a fluorogenic substrate, we showed that DADS increases caspase-3 activity in a time-dependent and concentration-dependent manner, in agreement with the report of Kwon et al. [43], which showed that DADS induced apoptosis in HL-60 and could block all features of apoptosis by z-VAD-fmk [43]. Bcl-2 down-regulation, Bax translocation, cytochrome *c* release into the cytosol and activation of caspase-9 and caspase-3 after DADS treatment in tumor cells were committed to apoptosis through activation of the mitochondrial pathway. This result is in agreement with the studies performed by Filomeni et al. [24] in neuroblastoma cells. Relocalization of Bax from the cytosol to the mitochondria is an early event during DADS-induced apoptosis. This event occurs in close association with mitochondrial cytochrome *c* release, activation of caspase-9, processing and activation of caspase-3, resulting in apoptosis. In monitoring endogenous Bax localization during DADS-induced apoptosis, cytochrome *c* release was never observed in the absence of Bax translocation, thereby supporting a model in which Bax translocation precedes cytochrome *c* release. The association of the cytosolic cytochrome *c* with Apaf1 and pro-caspase-9 contributes to the formation of apoptosome, leading to activation of caspase-9 as observed by others [44], which then activates effector caspases such as caspase-3. Apparently, the present study demonstrated that DADS induced human tumor cells apoptosis via a promoted caspase-3 pathway [45].

In the future, studies focusing on cell signaling and the biological significance of DADS-induced apoptosis and cell cycle arrest would lead to the exploration of the mechanisms of chemotherapeutic potency of DADS in human cancer. Presumably, DADS triggers other signaling pathways, which remain to be determined. DADS induces apoptosis through the mitochondrial pathway, as evidenced by the loss of mitochondrial membrane potential and the release of mitochondrial cytochrome *c* (Fig. 3A and B). Based on the results of our investigation, we proposed a schematic model (Fig. 5) to show how DADS changed different molecular events, leading to apoptosis in human cancer cells. The proposed chain of events mediated particularly through the mitochondria is as follows: DADS induced Bax translocation from the cytosol to the mitochondria, and this in turn activated Bax to form Bax multimers in the mitochondria; Bax induces mitochondrial damage and releases cytochrome *c* and subsequent apoptosis through caspase-3.

5. Conclusions

Thus, the results of our study demonstrated that DADS, a major oil-soluble constituent of garlic, has apoptotic potential in cancer cells. Although the exact mechanism involved in their protective effects against carcinogenesis has not been clearly understood at present, our results suggested that the mechanism of apoptosis induced by DADS was regulated through a mitochondrial pathway targeted to caspase-3. Together, these results indicate that mitochondria certainly play a major role in DADS-induced apoptosis. This functional correlation may also be useful in the identification and/or synthesis of novel anticancer compounds. These findings suggest that DADS may provide a new and effective chemical class of anticancer agents and may prove to be an effective agent for cancer prevention.

References

[1] Herman-Antosiewicz A, Singh SV. Signal transduction pathways leading to cell cycle arrest and apoptosis induction in cancer cells by *Allium* vegetable-derived organosulfur compounds: a review. Mutat Res 2004;555:121–31.
[2] Karmakar S, Banik NL, Patel SJ, Ray SK. Garlic compounds induced calpain and intrinsic caspase cascade for apoptosis in human malignant neuroblastoma SH-SY5Y cells. Apoptosis 2007;12:671–84.
[3] Khanum F, Anilakumar KR, Viswanathan KR. Anticarcinogenic properties of garlic: a review. Crit Rev Food Sci Nutr 2004;44:479–88.
[4] Milner JA. A historical perspective on garlic and cancer. J Nutr 2001;131: 1027S–31S.
[5] Xiao D, Lew KL, Kim YA, Zeng Y, Hahm ER, Dhir R, Singh SV. Diallyl trisulfide suppresses growth of PC-3 human prostate cancer xenograft in vivo in association with Bax and Bak induction. Clin Cancer Res 2006;12:6836–43.
[6] Kim YA, Xiao D, Xiao H, Powolny AA, Lew KL, Reilly ML, Zeng Y, Wang Z, Singh SV. Mitochondria-mediated apoptosis by diallyl trisulfide in human prostate cancer cells is associated with generation of reactive oxygen species and regulated by Bax/Bak. Mol Cancer Ther 2007;6:1599–609.
[7] Pinto JT, Lapsia S, Shah A, Santiago H, Kim G. Antiproliferative effects of garlic-derived and other allium related compounds. In: Go VLW, editor. Nutrition and cancer prevention: new insights into the role of phytochemicals. Advances in experimental medicine and biology, Vol. 492. New York: Kluwer Academic/ Plenum; 2001. p. 83–106.
[8] Wu X, Kassie F, Mersch-Sundermann V. Induction of apoptosis in tumor cells by naturally occurring sulfur-containing compounds. Mutat Res 2005;589:81–102.
[9] Moroni MC, Hickman ES, Lazzerini Denchi E, Caprara G, Colli E, Cecconi F, Muller H, Helin K. Apaf-1 is a transcriptional target for E2F and p53. Nat Cell Biol 2001;3: 552–8.
[10] Gupta N, Porter TD. Garlic and garlic-derived compounds inhibit human squalene monooxygenase. J Nutr 2001;131:1662–7.
[11] Omkumar RV, Kadam SM, Banerji A, Ramasarma T. On the involvement of intramolecular protein disulfide in the irreversible inactivation of 3-hydroxy-3-methylglutaryl-CoA reductase by diallyl disulfide. Biochim Biophys Acta 1993; 1164:108–12.
[12] Herr I, Debatin KM. Cellular stress response and apoptosis in cancer therapy. Blood 2001;98:2603–14.
[13] Tsujimoto Y. Cell death regulation by the Bcl-2 protein family in the mitochondria. J Cell Physiol 2003;195:158–67.
[14] Hengartner MO. The biochemistry of apoptosis. Nature 2000;407:770–6.
[15] Borner C. The Bcl-2 protein family: sensors and checkpoints for life-or-death decisions. Mol Immunol 2003;39:615–47.
[16] Wolter KG, Hsu YT, Smith CL, Nechushtan A, Xi XG, Youle RJ. Movement of Bax from the cytosol to mitochondria during apoptosis. J Cell Biol 1997;139:1281–92.
[17] Kuwana T, Mackey MR, Perkins G, Ellisman MH, Latterich M, Schneiter R, Green DR, Newmeyer DD. Bid, Bax, and lipids cooperate to form supramolecular openings in the outer mitochondrial membrane. Cell 2002;111:331–42.
[18] Kroemer G, Galluzzi L, Brenner C. Mitochondrial membrane permeabilization in cell death. Physiol Rev 2007;87:99–163.
[19] Nechushtan A, Smith CL, Lamensdorf I, Yoon SH, Youle RJ. Bax and Bak coalesce into novel mitochondria-associated clusters during apoptosis. J Cell Biol 2001;153: 1265–76.
[20] De Oliveira F, Chauvin C, Ronot X, Mousseau M, Leverve X, Fontaine E. Effects of permeability transition inhibition and decrease in cytochrome *c* content on doxorubicin toxicity in K562 cells. Oncogene 2006;25:2646–55.
[21] Hanahan D, Weinberg RA. The hallmarks of cancer. Cell 2000;100:57–70.
[22] Brenner C, Grimm S. The permeability transition pore complex in cancer cell death. Oncogene 2006;25:4744–56.
[23] Galluzzi L, Larochette N, Zamzami N, Kroemer G. Mitochondria as therapeutic targets for cancer chemotherapy. Oncogene 2006;25:4812–30.
[24] Filomeni G, Aquilano K, Rotilio G, Ciriolo MR. Reactive oxygen species-dependent c-Jun NH_2-terminal kinase/c-Jun signaling cascade mediates neuroblastoma cell death induced by diallyl disulfide. Cancer Res 2003;63:5940–9.
[25] Nagaraj NS, Vigneswaran N, Zacharias W. Hypoxia inhibits TRAIL-induced tumor cell apoptosis: involvement of lysosomal cathepsins. Apoptosis 2007;12: 125–39.
[26] Parone PA, James DI, Da Cruz S, Mattenberger Y, Donze O, Barja F, Martinou JC. Inhibiting the mitochondrial fission machinery does not prevent Bax/Bak-dependent apoptosis. Mol Cell Biol 2006;26:7397–408.
[27] Nagaraj NS, Singh OV. Proteomic and genomic analysis of human tumor cells treated with diallyl disulfide. J Nutr 2007:290S.
[28] Gupta S. Molecular signaling in death receptor and mitochondrial pathways of apoptosis (Review). Int J Oncol 2003;22:15–20.
[29] Hickman ES, Helin K. The regulation of APAF1 expression during development and tumourigenesis. Apoptosis 2002;7:167–71.
[30] Riedl SJ, Shi Y. Molecular mechanisms of caspase regulation during apoptosis. Nat Rev Mol Cell Biol 2004;5:897–907.

[31] Pellecchia M, Reed JC. Inhibition of anti-apoptotic Bcl-2 family proteins by natural polyphenols: new avenues for cancer chemoprevention and chemotherapy. Curr Pharm Des 2004;10:1387–98.
[32] Sun SY, Hail Jr N, Lotan R. Apoptosis as a novel target for cancer chemoprevention. J Natl Cancer Inst 2004;96:662–72.
[33] Dausch JG, Nixon DW. Garlic: a review of its relationship to malignant disease. Prev Med 1990;19:346–61.
[34] Arunkumar A, Vijayababu MR, Gunadharini N, Krishnamoorthy G, Arunakaran J. Induction of apoptosis and histone hyperacetylation by diallyl disulfide in prostate cancer cell line PC-3. Cancer Lett 2007;251:59–67.
[35] Fortin A, Cregan SP, MacLaurin JG, Kushwaha N, Hickman ES, Thompson CS, Hakim A, Albert PR, Cecconi F, Helin K, et al. APAF1 is a key transcriptional target for p53 in the regulation of neuronal cell death. J Cell Biol 2001;155: 207–16.
[36] Chinnaiyan AM, O'Rourke K, Tewari M, Dixit VM. FADD, a novel death domain-containing protein, interacts with the death domain of Fas and initiates apoptosis. Cell 1995;81:505–12.
[37] Ohuchida K, Mizumoto K, Ohhashi S, Yamaguchi H, Konomi H, Nagai E, Yamaguchi K, Tsuneyoshi M, Tanaka M. S100A11, a putative tumor suppressor gene, is overexpressed in pancreatic carcinogenesis. Clin Cancer Res 2006;12: 5417–22.
[38] Lieuallen K, Pennacchio LA, Park M, Myers RM, Lennon GG. Cystatin B-deficient mice have increased expression of apoptosis and glial activation genes. Hum Mol Genet 2001;10:1867–71.
[39] Jo HJ, Song JD, Kim KM, Cho YH, Kim KH, Park YC. Diallyl disulfide induces reversible G2/M phase arrest on a p53-independent mechanism in human colon cancer HCT-116 cells. Oncol Rep 2008;19:275–80.
[40] Johnstone RW, Ruefli AA, Lowe SW. Apoptosis: a link between cancer genetics and chemotherapy. Cell 2002;108:153–64.
[41] Wallace-Brodeur RR, Lowe SW. Clinical implications of p53 mutations. Cell Mol Life Sci 1999;55:64–75.
[42] Bottone Jr FG, Baek SJ, Nixon JB, Eling TE. Diallyl disulfide (DADS) induces the antitumorigenic NSAID-activated gene (NAG-1) by a p53-dependent mechanism in human colorectal HCT 116 cells. J Nutr 2002;132:773–8.
[43] Kwon KB, Yoo SJ, Ryu DG, Yang JY, Rho HW, Kim JS, Park JW, Kim HR, Park BH. Induction of apoptosis by diallyl disulfide through activation of caspase-3 in human leukemia HL-60 cells. Biochem Pharmacol 2002;63:41–7.
[44] Zou H, Yang R, Hao J, Wang J, Sun C, Fesik SW, Wu JC, Tomaselli KJ, Armstrong RC. Regulation of the Apaf-1/caspase-9 apoptosome by caspase-3 and XIAP. J Biol Chem 2003;278:8091–8.
[45] Srinivasula SM, Ahmad M, Fernandes-Alnemri T, Alnemri ES. Autoactivation of procaspase-9 by Apaf-1-mediated oligomerization. Mol Cell 1998;1:949–57.